

# Gas dynamics and Heat and Mass Transfer

## Numerical Solution of the Convection–Diffusion Equations

Student: Pedro López Sancha

Professor: Carlos-David Pérez Segarra

Aerospace Technology Engineering  
The School of Industrial, Aerospace and Audiovisual Engineering of Terrassa  
Technic University of Catalonia

July 10, 2021



**UNIVERSITAT POLITÈCNICA DE CATALUNYA**  
**BARCELONATECH**

---

**Escola Superior d'Enginyeries Industrial,  
Aeroespacial i Audiovisual de Terrassa**



## Contents

<b>1</b>	<b>Introduction</b>	<b>2</b>
<b>2</b>	<b>The convection–diffusion equations</b>	<b>3</b>
2.1	Reynolds transport theorem . . . . .	3
2.2	Continuity equation . . . . .	3
2.3	Momentum equation . . . . .	3
2.4	Energy equation . . . . .	3
2.5	Species equation . . . . .	3
2.6	Convection–diffusion equations . . . . .	3
<b>3</b>	<b>Numerical study</b>	<b>4</b>
3.1	Assumptions . . . . .	4
3.2	Spatial discretization . . . . .	4
3.3	Time discretization . . . . .	5
3.4	Discretization of the continuity equation . . . . .	5
3.5	Discretization of the general convection–diffusion equation . . . . .	6
3.6	Evaluation of the convective terms . . . . .	8
3.6.1	Upwind–Difference Scheme (UDS) . . . . .	8
3.6.2	Central–Difference Scheme (CDS) . . . . .	9
3.6.3	Second–order Upwind Linear Extrapolation (SUDS) . . . . .	10
3.6.4	Quadratic Upwind Interpolation for Convective Kinematics (QUICK) . . . . .	12
3.6.5	Exponential–Difference Scheme (EDS) . . . . .	13
3.6.6	Normalization of variables . . . . .	14
3.6.7	High–order bounded convection schemes and SMART scheme . . . . .	14
3.6.8	Summary of schemes . . . . .	15

## **1 Introduction**

## 2 The convection–diffusion equations

### 2.1 Reynolds transport theorem

$$\frac{d}{dt} \int_{V(t)} F(\mathbf{x}, t) d\mathbf{x} = \int_{V(t)} \frac{\partial F}{\partial t} d\mathbf{x} + \int_{A(t)} F(\mathbf{x}, t) \mathbf{b} \cdot \mathbf{n} dS \quad (2.1)$$

### 2.2 Continuity equation

$$\frac{\partial \rho}{\partial t} + \nabla \cdot (\rho \mathbf{v}) = 0 \quad (2.2)$$

### 2.3 Momentum equation

$$\frac{\partial(\rho \mathbf{v})}{\partial t} + \nabla \cdot (\rho \mathbf{v} \otimes \mathbf{v}) = \nabla \cdot (\mu \nabla \mathbf{v}) + \{ \nabla \cdot (\tau - \mu \nabla \mathbf{v}) - \nabla p + \rho \mathbf{g} \} \quad (2.3)$$

### 2.4 Energy equation

$$\frac{\partial(\rho T)}{\partial t} + \nabla \cdot (\rho \mathbf{v} T) = \nabla \cdot \left( \frac{\lambda}{c_v} \nabla T \right) + \left\{ \frac{\tau \circ \nabla \mathbf{v} - \nabla \cdot \dot{\mathbf{q}}^R - p \nabla \cdot \mathbf{v}}{c_v} \right\} \quad (2.4)$$

### 2.5 Species equation

$$\frac{\partial(\rho Y_k)}{\partial t} + \nabla \cdot (\rho \mathbf{v} Y_k) = \nabla \cdot (\rho D_{km} \nabla Y_k) + \{ \dot{\omega}_k \} \quad (2.5)$$

### 2.6 Convection–diffusion equations

### 3 Numerical study

#### 3.1 Assumptions

In order to solve the convection–diffusion equations numerically, we must make some assumptions which will simplify our study.

1. The location where the problem takes place is a closed connected set  $K$  contained in a bounded open connected set  $\Omega \subset \mathbb{R}^m$ , where  $m = 1, 2, 3$  depends on the dimension of the problem. Both  $K$  and  $\Omega$  are  $\mathcal{C}^1$  or Lipschitz domains, allowing us to use vector calculus theorems.
2. The problem lasts for finite time, starting at time  $t = 0$  and ending at time  $t = t_{\max}$ . Therefore the time interval is  $I = (0, t_{\max}) \subset \mathbb{R}$ .
3. The closed connected set  $K$  can be expressed as the union of finitely many closed sets  $\mathcal{V}_1, \dots, \mathcal{V}_r$ , that is,  $K = \mathcal{V}_1 \cup \dots \cup \mathcal{V}_r$ . Moreover, these sets

The control volume centered at node  $P$  will be denoted by  $\mathcal{V}_P$ . Its boundary, known as the control surface, will be expressed as  $\mathcal{S}_P = \partial\mathcal{V}_P$ . The volume  $\mathcal{V}_P$  occupies in  $\mathbb{R}^m$

#### 3.2 Spatial discretization

The type of problems addressed in this project occur in a bounded domain  $\Omega \subset \mathbb{R}^m$  with  $1 \leq m \leq 3$  depending on the case. In order to solve the problem numerically, a control–volume formulation is followed. This methodology discretizes the domain into nonoverlapping control volumes along with a grid of points named discretization nodes. The resulting discretized domain is named mesh or numerical grid [1].

There exist several types of grids according to the shape of control volumes and the ammount of subdivisions the domain has been partitioned into [2]:

- Structured (regular) grid:
- Block–structured grid:
- Unstructured grid:

Hereinafter, a structured regular grid approach will be followed. This formulation allows for two manners to discretize the domain, namely, cell–centered and node–centered discretizations. The former places discretization nodes over the domain and generates a control–volume centered on each node. The latter first generates the control–volumes and then places a node at the center of each one.



**Figure 3.1.** A figure with two subfigures

### 3.3 Time discretization

### 3.4 Discretization of the continuity equation

As seen before, the continuity equation in differential form is

$$\frac{\partial \rho}{\partial t} + \nabla \cdot (\rho \mathbf{v}) = 0 \quad (\mathbf{x}, t) \in \Omega \times I \quad (3.1)$$

Since the above relation is true on  $\Omega \times I$ , fixing one time  $t \in I$  and integrating over a control volume  $\mathcal{V}_P \subset \Omega$  yields

$$\int_{\mathcal{V}_P} \frac{\partial \rho}{\partial t} d\mathbf{x} + \int_{\mathcal{V}_P} \nabla \cdot (\rho \mathbf{v}) d\mathbf{x} = 0 \quad (3.2)$$

Let  $\mathcal{S}_P = \partial \mathcal{V}_P$  be the control surface, i.e. the boundary of the control volume. Then applying the divergence theorem on the second term of equation (3.2),

$$\int_{\mathcal{V}_P} \frac{\partial \rho}{\partial t} d\mathbf{x} + \int_{\mathcal{S}_P} \rho \mathbf{v} \cdot \mathbf{n} dS = 0 \quad (3.3)$$

With the aim of simplifying the first term of (3.3), the average density of the control volume is defined as

$$\bar{\rho}_P = \frac{1}{V_P} \int_{\mathcal{V}_P} \rho d\mathbf{x} \quad (3.4)$$

Introducing this relation in equation (3.3),

$$\frac{d\bar{\rho}_P}{dt} V_P + \int_{\mathcal{S}_P} \rho \mathbf{v} \cdot \mathbf{n} dS = 0 \quad (3.5)$$

The mass flow term can be further simplified if a cartesian mesh is being used. In case of a 2D–mesh, the control surface can be partitioned into four different faces, namely, the east, west, north and south faces. In this context the control surface is  $\mathcal{S}_P = \mathcal{S}_{Pe} \cup \mathcal{S}_{Pw} \cup \mathcal{S}_{Pn} \cup \mathcal{S}_{Ps}$  and the mass flow term may be expressed as

$$\int_{\mathcal{S}_P} \rho \mathbf{v} \cdot \mathbf{n} dS = \sum_i \int_{\mathcal{S}_{Pi}} \rho \mathbf{v} \cdot \mathbf{n} dS = \dot{m}_e + \dot{m}_w + \dot{m}_n + \dot{m}_s \quad (3.6)$$

If a 3D–mesh is being used, the contributions of top and bottom faces must be considered. The control surface is the union  $\mathcal{S}_P = \mathcal{S}_{Pe} \cup \mathcal{S}_{Pw} \cup \mathcal{S}_{Pn} \cup \mathcal{S}_{Ps} \cup \mathcal{S}_{Pt} \cup \mathcal{S}_{Pb}$ , and therefore the mass flow incorporates two new terms

$$\int_{\mathcal{S}_P} \rho \mathbf{v} \cdot \mathbf{n} dS = \sum_i \int_{\mathcal{S}_{Pi}} \rho \mathbf{v} \cdot \mathbf{n} dS = \dot{m}_e + \dot{m}_w + \dot{m}_n + \dot{m}_s + \dot{m}_t + \dot{m}_b \quad (3.7)$$

This allows writing equation (3.5) in the following way:

$$\frac{d\bar{\rho}_P}{dt} V_P + \sum_i \dot{m}_i = 0 \quad (3.8)$$

The average density of the control volume is roughly the density at the discretization node, that is,  $\bar{\rho}_P \approx \rho_P$ . Integrating (3.8) over the time interval  $[t^n, t^{n+1}]$  gives

$$V_P \int_{t^n}^{t^{n+1}} \frac{d\bar{\rho}_P}{dt} dt + \int_{t^n}^{t^{n+1}} \sum_i \dot{m}_i dt = 0 \quad (3.9)$$

The first term of (3.9) has a straightforward simplification applying a corollary of the fundamental theorem of calculus. Regarding the second term, numerical integration is applied,

$$(\rho_P^{n+1} - \rho_P^n) V_P + \left( \beta \sum_i \dot{m}_i^{n+1} + (1 - \beta) \sum_i \dot{m}_i^n \right) (t^{n+1} - t^n) = 0 \quad (3.10)$$

where  $\beta \in \{0, \frac{1}{2}, 1\}$  depends on the chosen integration scheme. For the sake of simplicity, superindex  $n + 1$  shall be dropped and the time instant  $n$  will be denoted by the superindex 0. Assuming a uniform time step  $\Delta t$ , the resulting discretized continuity equation is

$$\frac{\rho_P - \rho_P^0}{\Delta t} V_P + \beta \sum_i \dot{m}_i + (1 - \beta) \sum_i \dot{m}_i^0 = 0 \quad (3.11)$$

### 3.5 Discretization of the general convection–diffusion equation

The generalized convection–diffusion for a real valued function  $\phi: \Omega \times I \subset \mathbb{R}^m \times \mathbb{R} \rightarrow \mathbb{R}$  is

$$\frac{\partial(\rho\phi)}{\partial t} + \nabla \cdot (\rho \mathbf{v} \phi) = \nabla \cdot (\Gamma_\phi \nabla \phi) + \dot{s}_\phi, \quad (\mathbf{x}, t) \in \Omega \times I \quad (3.12)$$

whereas for a vector valued function  $\phi = (\phi_1, \dots, \phi_m): \Omega \times I \subset \mathbb{R}^m \times \mathbb{R} \rightarrow \mathbb{R}^m$  it is written as

$$\frac{\partial(\rho\phi)}{\partial t} + \nabla \cdot (\rho \mathbf{v} \otimes \phi) = \nabla \cdot (\Gamma_\phi \nabla \phi) + \dot{s}_\phi, \quad (\mathbf{x}, t) \in \Omega \times I \quad (3.13)$$

where  $\otimes$  denotes the outer product of  $\mathbf{v}: \Omega \times I \subset \mathbb{R}^m \times \mathbb{R} \rightarrow \mathbb{R}^m$  and  $\phi$ , which is a  $m \times m$  matrix. Since the generalized convection–diffusion equation for a vector valued function actually comprises  $m$  equations, one for each component function, only the discretization for a real valued function will be studied.

Integrating (3.12) over  $\mathcal{V}_P \times [t^n, t^{n+1}] \subset \Omega \times I$  and using Fubini's theorem

$$\begin{aligned} \int_{t^n}^{t^{n+1}} \int_{\mathcal{V}_P} \frac{\partial(\rho\phi)}{\partial t} d\mathbf{x} dt + \int_{t^n}^{t^{n+1}} \int_{\mathcal{V}_P} \nabla \cdot (\rho \mathbf{v} \phi) d\mathbf{x} dt &= \\ &= \int_{t^n}^{t^{n+1}} \int_{\mathcal{V}_P} \nabla \cdot (\Gamma_\phi \nabla \phi) d\mathbf{x} dt + \int_{t^n}^{t^{n+1}} \int_{\mathcal{V}_P} \dot{s}_\phi d\mathbf{x} dt \end{aligned} \quad (3.14)$$

The simplification of the first term is analogous to that of the continuity equation. The average value of  $\rho\phi$  on  $\mathcal{V}_P$  at time  $t$  is defined by

$$(\rho\phi)_P = \frac{1}{V_P} \int_{\mathcal{V}_P} \rho\phi d\mathbf{x} \quad (3.15)$$

then

$$\int_{t^n}^{t^{n+1}} \int_{\mathcal{V}_P} \frac{\partial(\rho\phi)}{\partial t} d\mathbf{x} dt = \int_{t^n}^{t^{n+1}} \frac{d}{dt} \int_{\mathcal{V}_P} \rho\phi d\mathbf{x} dt = \int_{t^n}^{t^{n+1}} \frac{d(\rho\phi)_P}{dt} V_P dt = \left\{ (\rho\phi)_P - (\rho\phi)_P^0 \right\} V_P \quad (3.16)$$

Divergence theorem must be applied to simplify the convective contribution,

$$\int_{t^n}^{t^{n+1}} \int_{\mathcal{V}_P} \nabla \cdot (\rho \mathbf{v} \phi) d\mathbf{x} dt = \int_{t^n}^{t^{n+1}} \int_{S_P} \rho \phi \mathbf{v} \cdot \mathbf{n} dS dt = \int_{t^n}^{t^{n+1}} \sum_i \int_{S_{Pi}} \rho \phi \mathbf{v} \cdot \mathbf{n} dS dt \quad (3.17)$$



The value that  $\phi$  takes on  $\mathcal{S}_{Pi}$  can be approximated by its value at a representative point, for instance, the point at face center, that is to say,  $\phi \approx \phi_i$ . Therefore,

$$\begin{aligned} \int_{t^n}^{t^{n+1}} \sum_i \int_{\mathcal{S}_i} \rho \phi \mathbf{v} \cdot \mathbf{n} dS dt &\approx \int_{t^n}^{t^{n+1}} \sum_i \int_{\mathcal{S}_i} \rho \phi_i \mathbf{v} \cdot \mathbf{n} dS dt = \int_{t^n}^{t^{n+1}} \sum_i \dot{m}_i \phi_i dt = \\ &= \left\{ \beta \sum_i \dot{m}_i \phi_i + (1 - \beta) \sum_i \dot{m}_i^0 \phi_i^0 \right\} \Delta t \quad (3.18) \end{aligned}$$

For the third term,

$$\int_{t^n}^{t^{n+1}} \int_{\mathcal{V}_P} \nabla \cdot (\Gamma_\phi \nabla \phi) d\mathbf{x} dt = \int_{t^n}^{t^{n+1}} \int_{\mathcal{S}_P} \Gamma_\phi \nabla \phi \cdot \mathbf{n} dS dt = \int_{t^n}^{t^{n+1}} \sum_i \int_{\mathcal{S}_{Pi}} \Gamma_\phi \nabla \phi \cdot \mathbf{n} dS dt \quad (3.19)$$

Since a cartesian mesh is being used, the outer normal vector to the face  $\mathcal{S}_{Pi}$  is constant and points in the direction of some coordinate axis. Hence the dot product  $\nabla \phi \cdot \mathbf{n}$  in the face  $\mathcal{S}_{Pi}$  equals the partial derivative with respect to  $x_i$  times  $\pm 1$ , depending on the direction of  $\mathbf{n}$ . For east, north and top faces the sign is positive, whilst for west, south and bottom faces the sign is negative. Again,  $\Gamma_\phi$  will be approximated by the value at the face center, and partial derivatives will be approximated by a finite centered difference. In order to simplify the notation, subindex  $\phi$  in the diffusion coefficient  $\Gamma_\phi$  will be dropped. For short, the following magnitudes are defined

$$D_i = \frac{\Gamma_i S_i}{d_{PI}} \quad (3.20)$$

$$D_i^0 = \frac{\Gamma_i^0 S_i}{d_{PI}} \quad (3.21)$$

where  $i$  and  $I$  refer to the face letter. For a 2D-mesh, equation (3.19) results in

$$\begin{aligned} \int_{t^n}^{t^{n+1}} \sum_i \int_{\mathcal{S}_{Pi}} \Gamma_\phi \nabla \phi \cdot \mathbf{n} dS dt &\approx \\ &\approx \int_{t^n}^{t^{n+1}} \left\{ D_i(\phi_E - \phi_P) - D_w(\phi_P - \phi_W) + D_n(\phi_N - \phi_P) - D_s(\phi_P - \phi_S) \right\} dt \approx \\ &\approx \beta \left\{ D_e(\phi_E - \phi_P) - D_w(\phi_P - \phi_W) + D_n(\phi_N - \phi_P) - D_s(\phi_P - \phi_S) \right\} \Delta t + \\ &+ (1 - \beta) \left\{ D_e^0(\phi_E - \phi_P) - D_w^0(\phi_P - \phi_W) + D_n^0(\phi_N - \phi_P) - D_s^0(\phi_P - \phi_S) \right\} \Delta t \quad (3.22) \end{aligned}$$

In the case of a 3D-mesh, the contributions of top and bottom faces must be accounted for.

In order to discretize the fourth term, the mean value of the source in  $\mathcal{V}_P$  at time  $t$  is by

$$\bar{s}_\phi = \frac{1}{V_P} \int_{\mathcal{V}_P} \dot{s}_\phi d\mathbf{x} \quad (3.23)$$

If the value of  $s_\phi$  is known, the relation  $\bar{s}_\phi = \dot{s}_\phi$  is true. Indeed,

$$\dot{s}_\phi = \frac{d}{dt} \bar{s}_\phi = \frac{1}{V_P} \frac{d}{dt} \int_{\mathcal{V}_P} s_\phi d\mathbf{x} = \frac{1}{V_P} \int_{\mathcal{V}_P} \dot{s}_\phi d\mathbf{x} = \bar{s}_\phi \quad (3.24)$$

In most cases, the dependence of  $\dot{s}_\phi$  on  $\phi$  is complicated. Since the equations obtained until now are linear, the relation between the source term and the variable would ideally be linear. This linearity is imposed as follows

$$\dot{s}_\phi = S_C^\phi + S_P^\phi \phi_P \quad (3.25)$$

where the values of  $S_C^\phi$  and  $S_P^\phi$  may vary with  $\phi$  [1]. Making use of these relations, the source term integral is discretized as

$$\int_{t^n}^{t^{n+1}} \int_{V_P} \dot{s}_\phi \, d\mathbf{x} \, dt = \int_{t^n}^{t^{n+1}} \dot{\bar{s}}_{\phi P} V_P \Delta t = (S_C^\phi + S_P^\phi \phi_P) V_P \Delta t \quad (3.26)$$

As shall be discussed later,  $S_P^\phi$  must be non-positive.

Finally, the discretization of the 2D generalized convection–diffusion equation is

$$\begin{aligned} & \frac{(\rho\phi)_P - (\rho\phi)_P^0}{\Delta t} V_P + \\ & + \beta (\dot{m}_e \phi_e - \dot{m}_w \phi_w + \dot{m}_n \phi_n - \dot{m}_s \phi_s) + (1 - \beta) (\dot{m}_e^0 \phi_e^0 - \dot{m}_w^0 \phi_w^0 + \dot{m}_n^0 \phi_n^0 - \dot{m}_s^0 \phi_s^0) = \\ & = \beta \{ D_e(\phi_E - \phi_P) - D_w(\phi_P - \phi_W) + D_n(\phi_N - \phi_P) - D_s(\phi_P - \phi_S) \} + \\ & + (1 - \beta) \{ D_e^0(\phi_E^0 - \phi_P^0) - D_w^0(\phi_P^0 - \phi_W^0) + D_n^0(\phi_N^0 - \phi_P^0) - D_s^0(\phi_P^0 - \phi_S^0) \} + \\ & + (S_C^\phi + S_P^\phi \phi_P) V_P \end{aligned} \quad (3.27)$$

### 3.6 Evaluation of the convective terms

The discretized convection–diffusion equations requires the values of certain variables at points different from the nodes. In this section several methods to compute  $\phi$  at faces are given. The values of  $\rho$  and  $\Gamma$  will be assumed to be known at the nodal points. East face will be taken as reference for simplicity. The generalization to the remaining faces is straightforward.

#### 3.6.1 Upwind–Difference Scheme (UDS)

Incompressible flows and gases at low Mach number are more influenced by upstream conditions than downstream conditions. Let  $(\mathbf{v} \cdot \mathbf{n})_e$  denote the value of the dot product  $\mathbf{v} \cdot \mathbf{n}$  at east face  $\mathcal{S}_{Pe}$ . If  $(\mathbf{v} \cdot \mathbf{n})_e > 0$ , fluid flows from node  $P$  to node  $E$ , hence  $P$  is the upstream node and  $E$  is the downstream node. Conversely, if  $(\mathbf{v} \cdot \mathbf{n})_e < 0$ , nodes interchange their roles as fluid flows from node  $E$  to node  $P$ . This situation is pictured in figures 3.2 and 3.3.

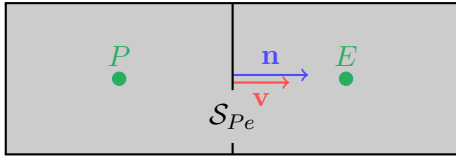


**Figure 3.2.** Since  $(\mathbf{v} \cdot \mathbf{n})_e > 0$  fluid flows from node  $P$  (upstream node) to node  $E$  (downstream node).

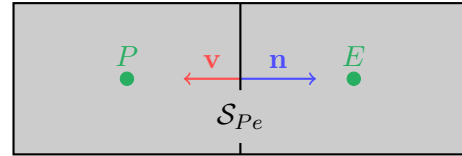


**Figure 3.3.** Since  $(\mathbf{v} \cdot \mathbf{n})_e < 0$  fluid flows from node  $E$  (upstream node) to node  $P$  (downstream node).

If  $(\mathbf{v} \cdot \mathbf{n})_e = 0$ , it implies  $\mathbf{v}_e$  lies in the orthogonal subspace to the vector space generated by  $\mathbf{n}$ . As a result, given the approximations taken, there is no fluid flow through face  $\mathcal{S}_{Pe}$ .

The Upwind–Difference Scheme assigns  $\phi_e$  the value of  $\phi$  at the upstream node, that is,

$$\phi_e^{\text{UDS}} = \begin{cases} \phi_P & \text{if } (\mathbf{v} \cdot \mathbf{n})_e > 0 \\ \phi_E & \text{if } (\mathbf{v} \cdot \mathbf{n})_e < 0 \end{cases} \quad (3.28)$$

This can be expressed in a more compact form as follows

$$\dot{m}_e(\phi_e - \phi_P) = \frac{\dot{m}_e - |\dot{m}_e|}{2}(\phi_E - \phi_P) \quad (3.29)$$

since the approximation to compute  $\dot{m}_e$  is related to  $(\mathbf{v} \cdot \mathbf{n})_e$  through the relation  $\dot{m}_e = (\mathbf{v} \cdot \mathbf{n})_e S_{Pe}$ . The scheme is shown in figures 3.4 and 3.5.

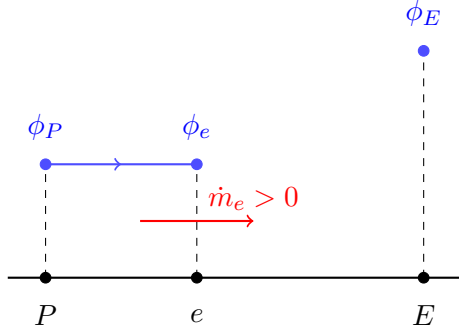


**Figure 3.4.** UDS when  $(\mathbf{v} \cdot \mathbf{n})_e > 0$ .

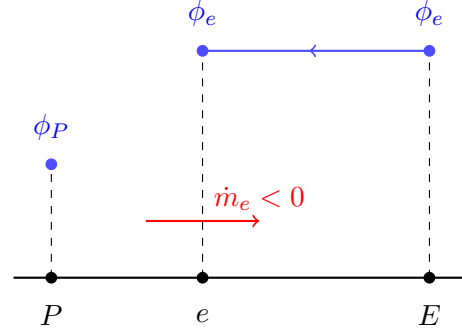


**Figure 3.5.** UDS when  $(\mathbf{v} \cdot \mathbf{n})_e < 0$ .

UDS is a stable scheme, however it suffers from numerical diffusion. Indeed, assuming the upstream node is  $P$ , expanding  $\phi$  about point  $x_P$  in its Taylor expansion up to 2<sup>nd</sup> degree and using Lagrange's remainder,

$$\phi_e = \phi_P + \left(\frac{\partial \phi}{\partial x}\right)_P d_{Pe} + \left(\frac{\partial^2 \phi}{\partial x^2}\right)_{\xi_1} \frac{d_{Pe}^2}{2} \quad (3.30)$$

it is apparent that UDS retains the first term on the left-hand side of (3.30). As a consequence, the highest order term of the error is  $(\partial_x \phi)_P d_{Pe}$ , which is proportional to the distance between  $P$  and the face  $S_{Pe}$ . This term resembles to a diffusion flux given, for instance, by Fourier's or Fick's laws of diffusion. The same result is obtained when  $E$  is the upstream node,

$$\phi_e = \phi_E - \left(\frac{\partial \phi}{\partial x}\right)_E d_{Ee} + \left(\frac{\partial^2 \phi}{\partial x^2}\right)_{\xi_2} \frac{d_{Ee}^2}{2} \quad (3.31)$$

whence it can be deduced that the error is bounded by  $\max\{ |(\partial_x \phi)_E d_{Pe}|, |(\partial_x \phi)_E d_{Ee}| \}$ . The numerical diffusion issue is magnified in multidimensional problems, where peaks of rapid variation can be obtained, hence very fine grids are required.

### 3.6.2 Central–Difference Scheme (CDS)

The Central–Difference Scheme assumes a linear distribution for  $\phi$  as illustrated in figure 3.6,

Thereby  $\phi_e$  can be obtained interpolating between  $\phi_P$  and  $\phi_E$ ,

$$\phi_e - \phi_P = f_e (\phi_E - \phi_P), \quad f_e = \frac{d_{Pe}}{d_{Pe} + d_{Ee}} \quad (3.32)$$

This yields a 2<sup>nd</sup> order approximation for  $\phi_e$  if  $d_{Pe} = d_{Ee}$ . In effect, applying Taylor's theorem about point  $x_e$ ,

$$\phi_P = \phi_e - \left(\frac{\partial \phi}{\partial x}\right)_e d_{Pe} + \frac{1}{2} \left(\frac{\partial^2 \phi}{\partial x^2}\right)_e d_{Pe}^2 + \frac{1}{6} \left(\frac{\partial^3 \phi}{\partial x^3}\right)_{\xi_1} d_{Pe}^3 \quad (3.33)$$

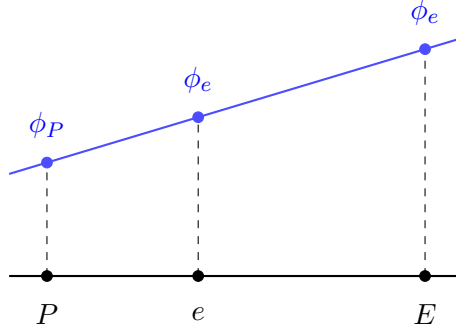


**Figure 3.6.** Central Difference Scheme (CDS).

The 2<sup>nd</sup> order approximation of  $(\partial_x \phi)_e$  is given by

$$\left(\frac{\partial \phi}{\partial x}\right)_e = \frac{\phi_E - \phi_P}{d_{PE}} - \left(\frac{\partial^3 \phi}{\partial x^3}\right)_{\xi_2} \frac{d_{PE}^2}{3!} = \frac{\phi_E - \phi_P}{d_{PE}} - \left(\frac{\partial^3 \phi}{\partial x^3}\right)_{\xi_2} \frac{(d_{Pe} + d_{Ee})^2}{3!} \quad (3.34)$$

Introducing (3.34) in (3.33) and imposing  $d_{Pe} = d_{Ee}$ ,

$$\phi_e - \phi_P = \frac{d_{Pe}}{d_{PE}}(\phi_E - \phi_P) - \left(\frac{\partial^2 \phi}{\partial x^2}\right)_e \frac{d_{Pe}^2}{2} - \left\{ \left(\frac{\partial^3 \phi}{\partial x^3}\right)_{\xi_1} + 4 \left(\frac{\partial^3 \phi}{\partial x^3}\right)_{\xi_2} \right\} \frac{d_{Pe}^3}{6} \quad (3.35)$$

As CDS retains the first term on the left-hand side of (3.35), the highest order term of the error is  $\frac{1}{2}(\partial_x^2 \phi)_e d_{Pe}^2$ , proving that CDS provides a 2<sup>nd</sup> order approximation of  $\phi_e$  when  $d_{Pe} = d_{Ee}$ . Nonetheless, this scheme is prone to stability problems producing oscillatory outputs since the approximation is of order higher than 1.

### 3.6.3 Second-order Upwind Linear Extrapolation (SUDS)

As stated previously, incompressible flows and fluids at low Mach number are more influenced by upstream condition than downstream conditions. In order to account for this fact and to ease the study, some notation is introduced. Located at the face separating two control volumes,  $f$  refers to the face,  $D$  is the downstream node,  $C$  is the first upstream node and  $U$  is the most upstream node. Some books may use  $U$  and  $UU$  instead of  $C$  and  $U$ , respectively.

The Second-order Upwind Linear Extrapolation scheme takes profit of this idea since it extrapolates  $\phi_e$  using a straight line between the values of  $\phi$  at nodes  $C$  and  $U$ . The two possible situations are pictured in figures 3.7 and 3.8.

On the one hand, when  $(\mathbf{v} \cdot \mathbf{n})_e > 0$ , the line between points  $(x_W, \phi_W)$  and  $(x_P, \phi_P)$  is given by

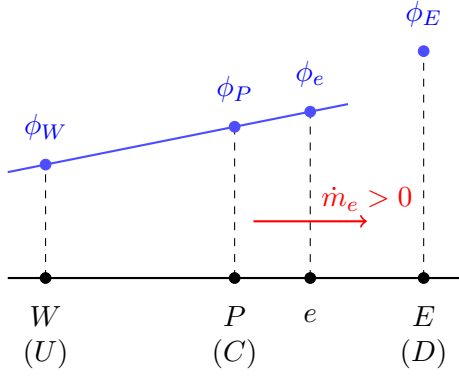
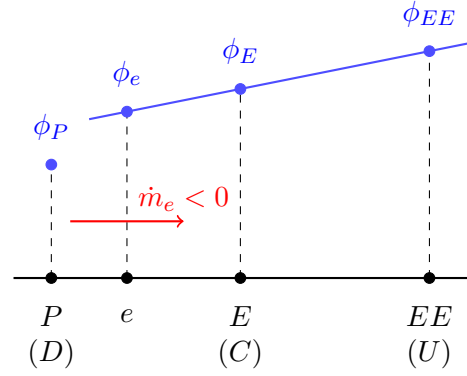
$$\phi(x) = \phi_W + \frac{\phi_P - \phi_W}{d_{PW}}(x - x_W) \quad (3.36)$$

and substituting at  $x = x_e$ , the formula for  $\phi_e$  is obtained:

$$\phi_e = \phi(x_e) = \phi_W + \frac{\phi_P - \phi_W}{d_{PW}}(x_e - x_W) = \phi_P + \frac{d_{Pe}}{d_{PW}}(\phi_P - \phi_W) \quad (3.37)$$

On the other hand, in the case of  $(\mathbf{v} \cdot \mathbf{n})_e < 0$ , the line between points  $(x_E, \phi_E)$  and  $(x_{EE}, \phi_{EE})$  is

$$\phi(x) = \phi_E + \frac{\phi_{EE} - \phi_E}{d_{E,EE}}(x - x_E) \quad (3.38)$$

**Figure 3.7.** SUDS when  $(\mathbf{v} \cdot \mathbf{n})_e > 0$ .**Figure 3.8.** SUDS when  $(\mathbf{v} \cdot \mathbf{n})_e < 0$ .

and the approximation of  $\phi_e$  is

$$\phi_e = \phi(x_e) = \phi_E + \frac{\phi_{EE} - \phi_E}{d_{E,EE}}(x_e - x_E) = \phi_E + \frac{d_{Ee}}{d_{E,EE}}(\phi_{EE} - \phi_E) \quad (3.39)$$

Using the new notation, (3.37) and (3.39) are both rewritten in the following manner:

$$\phi_f - \phi_C = \frac{d_{Cf}}{d_{CU}}(\phi_C - \phi_U) \quad (3.40)$$

In order to prove that SUDS is a second order scheme when a locally uniform mesh is used and  $(\mathbf{v} \cdot \mathbf{n})_e > 0$ , consider the Taylor expansion up to  $2^{nd}$  degree of  $\phi$  about point  $x_W$ ,

$$\phi_e = \phi_W + \left(\frac{\partial \phi}{\partial x}\right)_W d_{We} + \left(\frac{\partial^2 \phi}{\partial x^2}\right)_{\xi_1} \frac{d_{We}^2}{2} \quad (3.41)$$

The first derivative of  $\phi$  with respect to  $x$  can be replaced by its first order approximation, namely,

$$\left(\frac{\partial \phi}{\partial x}\right)_W = \frac{\phi_P - \phi_W}{d_{PW}} - \left(\frac{\partial^2 \phi}{\partial x^2}\right)_{\xi_2} \frac{d_{PW}}{2} \quad (3.42)$$

thereby,

$$\begin{aligned} \phi_e &= \phi_W + \frac{d_{We}}{d_{PW}}(\phi_P - \phi_W) + \left(\frac{\partial^2 \phi}{\partial x^2}\right)_{\xi_1} \frac{d_{We}^2}{2} - \left(\frac{\partial^2 \phi}{\partial x^2}\right)_{\xi_2} \frac{d_{We} d_{PW}}{2} \\ &= \phi_P + \frac{d_{Pe}}{d_{PW}}(\phi_P - \phi_W) + \left(\frac{\partial^2 \phi}{\partial x^2}\right)_{\xi_1} \frac{(d_{PW} + d_{Pe})^2}{2} - \left(\frac{\partial^2 \phi}{\partial x^2}\right)_{\xi_2} \frac{(d_{PW} + d_{Pe}) d_{PW}}{2} \end{aligned} \quad (3.43)$$

The scheme retains the two first terms on the right-hand side of (3.43), therefore the error is composed by the last two terms. The locally uniform mesh hypothesis implies  $d_{PW} = 2d_{Pe} = L$ , therefore the error term is multiplied by  $L^2$ ,

$$\phi_e = \phi_P + \frac{d_{Pe}}{d_{PW}}(\phi_P - \phi_W) + \frac{3L^2}{4} \left\{ 3 \left(\frac{\partial^2 \phi}{\partial x^2}\right)_{\xi_1} - \left(\frac{\partial^2 \phi}{\partial x^2}\right)_{\xi_2} \right\} \quad (3.44)$$

whence the second order of SUDS is deduced. The proof in the case of  $(\mathbf{v} \cdot \mathbf{n})_e < 0$  is analogous.

### 3.6.4 Quadratic Upwind Interpolation for Convective Kinematics (QUICK)

A logical improvement of CDS is using a parabola to interpolate between nodal points rather than a straight line. To construct a parabola three points are needed. As aforementioned, upstream conditions have a greater influence on flow properties than downstream conditions for incompressible flows and low Mach number gases. QUICK scheme takes profit of this fact.

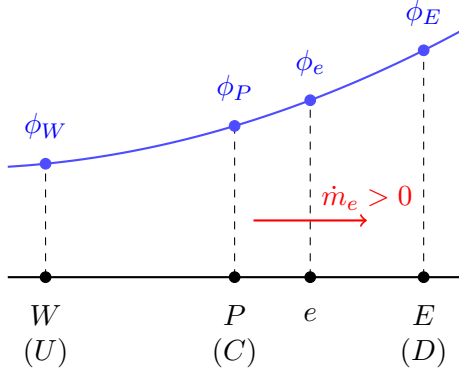


**Figure 3.9.** QUICK when  $(\mathbf{v} \cdot \mathbf{n})_e > 0$ .

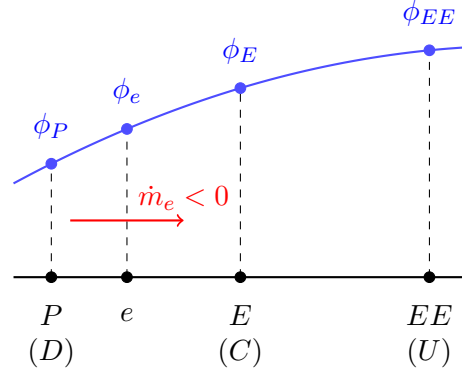


**Figure 3.10.** QUICK when  $(\mathbf{v} \cdot \mathbf{n})_e < 0$ .

Let  $(x_0, \phi_0)$ ,  $(x_1, \phi_1)$ ,  $(x_2, \phi_2)$  be the points which the polynomial  $p(x)$  must interpolate, that is,  $p(x_0) = \phi_0$ ,  $p(x_1) = \phi_1$  and  $p(x_2) = \phi_2$ , satisfying  $x_0 < x_1 < x_2$ . If  $(\mathbf{v} \cdot \mathbf{n})_e > 0$  then  $x_0 = x_W$ ,  $x_1 = x_P$  and  $x_2 = x_E$ , whereas  $x_0 = x_P$ ,  $x_1 = x_E$  and  $x_2 = x_{EE}$  in case of  $(\mathbf{v} \cdot \mathbf{n})_e < 0$ . Let  $p(x)$  be the following polynomial

$$p(x) = a_0 + a_1(x - x_0) + a_2(x - x_0)(x - x_1), \quad a_0, a_1, a_2 \in \mathbb{R} \quad (3.45)$$

Since the interpolating polynomial exists and is unique [referencia](#), by imposing the interpolating condition,  $p(x)$  will be the desired polynomial. The interpolating condition is,

$$\left. \begin{aligned} p(x_0) &= a_0 = \phi_0 \\ p(x_1) &= a_0 + a_1(x_1 - x_0) = \phi_1 \\ p(x_2) &= a_0 + a_1(x_2 - x_0) + a_2(x_2 - x_0)(x_2 - x_1) = \phi_2 \end{aligned} \right\} \quad (3.46)$$

which yields the following linear system:

$$\begin{pmatrix} 1 & 0 & 0 \\ 1 & x_1 - x_0 & 0 \\ 1 & x_2 - x_0 & (x_2 - x_1)(x_2 - x_0) \end{pmatrix} \begin{pmatrix} a_0 \\ a_1 \\ a_2 \end{pmatrix} = \begin{pmatrix} \phi_0 \\ \phi_1 \\ \phi_2 \end{pmatrix} \quad (3.47)$$

The determinant of the system matrix is non-zero because the abscissae are distinct, therefore the solution is given by

$$\left. \begin{aligned} a_0 &= \phi_0 \\ a_1 &= \frac{\phi_1 - \phi_0}{x_1 - x_0} \\ a_2 &= \frac{\phi_2 - \phi_0}{(x_2 - x_1)(x_2 - x_0)} - \frac{\phi_1 - \phi_0}{(x_2 - x_1)(x_1 - x_0)} \end{aligned} \right\} \quad (3.48)$$

and the polynomial is

$$p(x) = \phi_0 - \frac{(x - x_2)(x - x_0)}{(x_2 - x_1)(x_1 - x_0)}(\phi_1 - \phi_0) + \frac{(x - x_1)(x - x_0)}{(x_2 - x_1)(x_2 - x_0)}(\phi_2 - \phi_0) \quad (3.49)$$

Assuming a uniform grid, i.e.  $x_1 - x_0 = x_2 - x_1 = L$  and the face  $f$  located at the midpoint between nodal points, the approximation of  $\phi_e$  given by QUICK scheme is

$$\phi_e = -\frac{1}{8}\phi_0 + \frac{6}{8}\phi_1 + \frac{3}{8}\phi_2 \quad (3.50)$$

and depending on the sign of  $(\mathbf{v} \cdot \mathbf{n})_e$ ,

$$\phi_e = \begin{cases} -\frac{1}{8}\phi_U + \frac{6}{8}\phi_C + \frac{3}{8}\phi_D & \text{if } (\mathbf{v} \cdot \mathbf{n})_e > 0 \\ -\frac{1}{8}\phi_D + \frac{6}{8}\phi_C + \frac{3}{8}\phi_U & \text{if } (\mathbf{v} \cdot \mathbf{n})_e < 0 \end{cases} \quad (3.51)$$

The output (3.51) provided by QUICK scheme is second-order accurate.

### 3.6.5 Exponential–Difference Scheme (EDS)

The exponential difference scheme assumes a distribution for  $\phi$  based on the steady 2–dimensional generalized convection–diffusion equation with no source term, that is to say,

$$\frac{d}{dx}(\rho u \phi) = \frac{d}{dx} \left( \Gamma \frac{d\phi}{dx} \right) \quad (3.52)$$

where  $u$  is the component of  $\mathbf{v}$  in the  $x$  direction. So as to ease the study,  $\rho u$  and  $\Gamma$  are assumed to be constant. Thereby the initial value problem obtained is

$$\begin{cases} \frac{d^2\phi}{dx^2} - \frac{\rho u}{\Gamma} \frac{d\phi}{dx} = 0 & \text{in } (x_P, x_E) \\ \phi(x_P) = \phi_P \\ \phi(x_E) = \phi_E \end{cases} \quad (3.53)$$

Since (3.53) is a second order linear ODE with two boundary conditions, its solutions exists, is unique, and is given by

$$\phi(x) = \phi_P - \frac{\phi_E - \phi_P}{e^{\frac{\rho u}{\Gamma} d_{PE}} - 1} + \frac{\phi_E - \phi_P}{e^{\frac{\rho u}{\Gamma} d_{PE}} - 1} e^{\frac{\rho u}{\Gamma} (x - x_P)} \quad (3.54)$$

Péclet’s number for heat transfer is defined as the following ratio,

$$\text{Pe} = \frac{\text{convection transport}}{\text{heat transport}} = \frac{\rho u L}{\lambda / c_p} \quad (3.55)$$

where  $L$  is a characteristic length of the problem. Since  $\lambda / c_p$  is the diffusion coefficient in equation (2.4), it can be substituted by the diffusion coefficient  $\Gamma$  of the generalized convection–diffusion equation, providing a new definition for Péclet’s number

$$\text{Pe} = \frac{\rho u L}{\Gamma} \quad (3.56)$$

Taking  $d_{PE}$  as characteristic length and evaluating (3.54) at  $x = x_e$ , the approximation of  $\phi_e$  given by EDS in terms of Péclet’s number is written as

$$\frac{\phi_e - \phi_P}{\phi_E - \phi_P} = \frac{e^{\text{Pe} \frac{d_{PE}}{L}} - 1}{e^{\text{Pe}} - 1} \quad (3.57)$$

### 3.6.6 Normalization of variables

Owing to numerical reasons, it is convenient to normalize spatial and convective variables, that is to say, define new variables which take a rather small range of values. This is accomplished using the *DCU* notation and defining

$$\hat{x} = \frac{x - x_U}{x_D - x_U}$$

$$\hat{\phi} = \frac{\phi - \phi_U}{\phi_D - \phi_U}$$

Of course,  $(\hat{x}_U, \hat{\phi}_U) = (0, 0)$ ,  $(\hat{x}_D, \hat{\phi}_D) = (1, 1)$  and  $\hat{x}_C, \hat{x}_f \in (0, 1)$ . However,  $\hat{\phi}$  is not necessarily in  $[0, 1]$  for all  $x \in [0, 1]$ , nor does it have to be an increasing function. These situations are represented in figures 3.11 and 3.12.

The normalized variable  $\hat{\phi}_f$  can be computed directly as shown in section referencia sección posterior and, based on this, the variable at face,

$$\phi_f = \phi_U + \hat{\phi}_f(\phi_D - \phi_U) \quad (3.58)$$

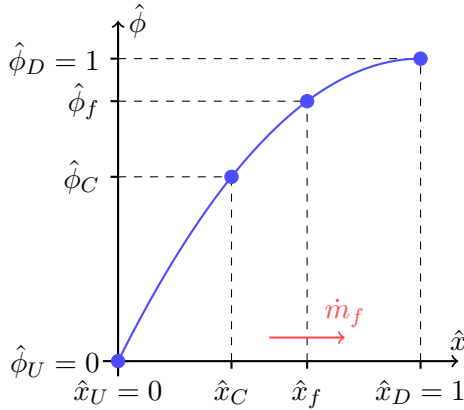


**Figure 3.11.** Scheme of normalized variables when  $\hat{\phi}(x)$  is a strictly increasing function.

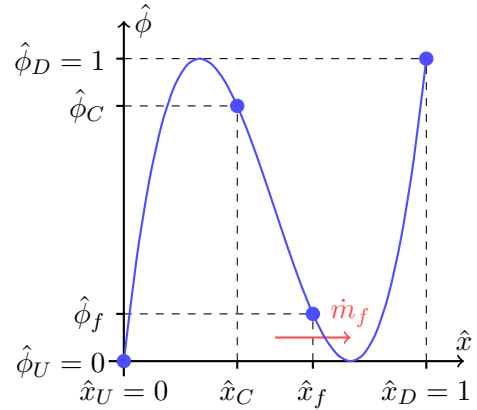


**Figure 3.12.** Scheme of normalized variables when  $\hat{\phi}(x)$  is not a strictly increasing function.

### 3.6.7 High–order bounded convection schemes and SMART scheme

As aforementioned, schemes whose order is higher than one might be unstable, producing oscillatory outputs for the convective variables. For instance, CDS, SUDS and QUICK are not bounded schemes. The conditions for stability and accuracy are formulated in [3]:

- (i)  $\hat{\phi}_f$  must be a continuous function of  $\hat{\phi}_C$ .
- (ii) If  $\hat{\phi}_C = 0$ , then  $\hat{\phi}_f = 0$ .
- (iii) If  $\hat{\phi}_C = 1$ , then  $\hat{\phi}_f = 1$ .
- (iv) If  $0 < \hat{\phi}_f < 1$ , then  $\hat{\phi}_C < \hat{\phi}_f < 1$ .

Conditions (i) through (iv) are represented in figure 3.13. A bounded convective scheme must output results lying within the shadowed region.



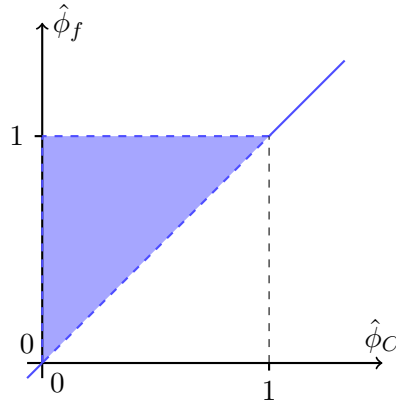


**Figure 3.13.** High-order bounded convection schemes conditions for stability.

The SMART scheme (Sharp and Monotonic Algorithm for Realistic Transport) is a bounded convective scheme [3], given by:

$$\hat{\phi}_f = \begin{cases} -\frac{\hat{x}_f(1 - 3\hat{x}_C + 2\hat{x}_f)}{\hat{x}_C(\hat{x}_C - 1)}\hat{\phi}_C & \text{if } 0 < \hat{\phi}_C < \frac{\hat{x}_C}{3} \\ \frac{\hat{x}_f(\hat{x}_f - \hat{x}_C)}{1 - \hat{x}_C} + \frac{\hat{x}_f(\hat{x}_f - 1)}{\hat{x}_C(\hat{x}_C - 1)}\hat{\phi}_C & \text{if } \frac{\hat{x}_C}{3} < \hat{\phi}_C < \frac{\hat{x}_C(1 + \hat{x}_f - \hat{x}_C)}{\hat{x}_f} \\ 1 & \text{if } \frac{\hat{x}_C(1 + \hat{x}_f - \hat{x}_C)}{\hat{x}_f} < \hat{\phi}_C < 1 \\ \hat{\phi}_C & \text{otherwise} \end{cases} \quad (3.59)$$

### 3.6.8 Summary of schemes

Below a summary of the studied schemes is shown:

Scheme	Face value
--------	------------

## References

- [1] Suhas V Patankar. *Numerical heat transfer and fluid flow*. McGraw–Hill Book Company, 1980.
- [2] Joel H Ferziger, Milovan Perić, and Robert L Street. *Computational methods for fluid dynamics*. Springer, 2002.
- [3] PH Gaskell and AKC Lau. “Curvature-compensated convective transport: SMART, a new boundedness-preserving transport algorithm”. In: *International Journal for numerical methods in fluids* 8.6 (1988), pp. 617–641.